Regenerative Therapy 26 (2024) 683–692

Contents lists available at ScienceDirect

Regenerative Therapy

journal homepage: http://www.elsevier.com/locate/reth

Original Article

Developing engineered muscle tissues utilizing standard cell culture plates and mesenchymal stem cell-conditioned medium

Yihao Wen [a, b, c], Jia Tian [b, c, d], Juan Li [b, c], Xiangming Na [b, c], Ziyi Yu [a, *], Weiqing Zhou [b, c, d, **]

[a] State Key Laboratory of Materials-Oriented Chemical Engineering, College of Chemical Engineering, Nanjing Tech University, Nanjing 211816, China
[b] State Key Laboratory of Biochemical Engineering, Institute of Process Engineering, Chinese Academy of Sciences, Beijing 100190, China
[c] Key Laboratory of Biopharmaceutical Preparation and Delivery, Chinese Academy of Sciences, Institute of Process Engineering, Beijing 100190, China
[d] College of Chemical Engineering, University of the Chinese Academy of Sciences, Beijing 101408, China

ARTICLE INFO

Article history:
Received 15 May 2024
Received in revised form
8 August 2024
Accepted 18 August 2024

Keywords:
Tissue engineering
Skeletal muscle
Myogenesis
Mesenchymal stem cells
Conditioned medium

ABSTRACT

The construction of engineered muscle tissues that resemble the function and microstructure of human muscles holds significant promise for various applications, including disease modeling, regenerative medicine, and biological machines. However, current muscle tissue engineering approaches often rely on complex equipment which may limit their accessibility and practicality. Herein, we present a convenient approach using a standard 24-well cell culture plate to construct a platform to facilitate engineered muscle tissues formation and culture. Using this platform, engineered muscle tissue with differentiation characteristics can be manufactured in large quantities. Additionally, the mesenchymal stem cell conditioned medium was utilized to promote the formation and functionality of the engineered muscle tissues. The resulting tissues comprised a higher cell density and a better differentiation effect in the tissues. Taken together, this study provides a simple, convenient, and effective platform for studying muscle tissue engineering.

1. Introduction

Skeletal muscle is vital to human physiology, enabling essential functions such as respiration and locomotion [1]. Its remarkable capacity for self-repair following minor injuries is facilitated by its inherent regenerative abilities [2]. However, severe injuries, particularly those accompanied by volumetric muscle loss (VML), can lead to permanent functional impairment [3]. Current therapies for VML are limited to autologous muscle transfers [4]. However, these approaches have limitations such as morbidity at the donor site, necrosis in the transplanted muscle, and restricted availability of tissues [5]. To overcome these limitations, tissue engineering has emerged as a viable alternative, providing the possibility to develop functional skeletal muscle tissue in vitro for transplantation.

Tissue engineering aims to mimic the structural and functional characteristics of natural skeletal muscle tissue [6]. This involves the alignment of myoblasts into parallel arrays, which is essential for generating force transmission within the muscle [2]. Therefore, engineered skeletal muscle tissue constructed through tissue engineering also requires terminal differentiation of myoblasts to fuse and form parallel arrangements to produce aligned structures [7]. While a variety of construction methods utilizing spatial constraints are used to achieve this alignment, such as electrospinning and 3D bioprinting, they suffer from obvious disadvantages of complex equipment and high cost. The molding method originated from the tendon structure, is a simpler method for constructing aligned skeletal muscle structures in vitro [8]. This method leverages the spatial constraint imposed by a mold to guide myoblasts alignment and fusing into myotubes [9]. For instance, Nenad Bursac used a customized nylon frame as a mold to produce highly aligned myotubes, which served as the foundation for engineered skeletal muscle with certain functions [10]. Despite these advancements,

* Corresponding author.
** Corresponding author. State Key Laboratory of Biochemical Engineering, Institute of Process Engineering, Chinese Academy of Sciences, Beijing 100190, China.
E-mail addresses: ziyi.yu@njtech.edu.cn (Z. Yu), wqzhou@ipe.ac.cn (W. Zhou).
Peer review under responsibility of the Japanese Society for Regenerative Medicine.

https://doi.org/10.1016/j.reth.2024.08.011

in vitro-cultured engineered skeletal muscle tissue still exhibits significant differences from their natural counterparts in terms of properties including myotube fusion index, muscle fiber length and width, etc. These differences are partly due to the current in vitro culture environments not fully replicating the complex physiological conditions of living organisms [11,12]. Therefore, while in vitro-generated engineered muscle tissue can mimic the structure of natural muscle tissue, it falls short in achieving comparable functional performance.

In this study, we introduce a smart and user-friendly engineered muscle tissue construction platform that circumvents the limitations of conventional electrospinning and 3D bioprinting techniques. This platform utilizes modified commercial 24-well cell culture plates to facilitate the construction of engineered skeletal muscle tissue under standard laboratory conditions, eliminating the need for complex and costly equipment. To improve the maturity and functionality of tissue-engineered skeletal muscle cultured in vitro, we leverage the paracrine effects of mesenchymal stem cell-conditioned medium. The medium is rich in factors and cytokines that support muscle cell differentiation and maturation, thus providing a more physiologically relevant environment for tissue engineering. This study provides a valuable tool for advancing the field of muscle tissue engineering.

2. Materials and methods

2.1. Materials

The main reagents used in this study were shown in Supplementary Table S1.

2.2. Cell culture

The mouse myoblast cell line C2C12 was obtained from the Haixing Biosciences and was used at passages 2 to 5. The growth medium (GM) for C2C12 was composed of DMEM basic and DMEM supplemented with 10% FBS and 1% P/S. The differentiation medium (DM) was composed of basic DMEM and DMEM supplemented with 2% HS and 1%P/S. The rabbit bone marrow mesenchymal stem cells (BM-MSCs) were obtained from Cyagen Biosciences and the growth medium was DMEM basic with 10% FBS and 1% P/S. Myoblasts and mesenchymal stem cells were cultured in a 5% CO_2 incubator at 37 °C and the medium was changed every other day.

2.3. MSC conditioned medium

MSCs (3×10^5 cells per well) were seeded on the surface of konjac glucomannan microcarriers (0.12 mL per well) and added to a 6 well plate with a low attachment surface. When the MSCs reached 80% confluence, cells were washed twice with PBS, and 3 mL/well of fresh serum-free medium was added. After a further 48 h incubation period, the conditioned medium was collected and centrifuged at 8000 rpm for 10 min to remove cell debris and passed through a 0.22 μm sterile filter. Then conditioned medium was stored at −80 °C until use.

2.4. Elisa

Quantitative concentrations of MSC secreted hepatocyte growth factor (HGF) and insulin-like growth factor (IGF) in conditioned media were determined using commercially available ELISA kits (R&D systems) and used according to the manufacturer's instructions.

2.5. Engineering muscle tissues fabrication platform

The PDMS anchors were designed using SolidWorks software (Dassault Systems). The female mold of the designed PDMS anchor point was made of polytetrafluoroethylene (PTFE) (Fig. 2a and Supplementary figure S1). The PDMS base and curing agents were well-mixed at a ratio of 10:1 and put into the vacuum oven to remove air bubbles. Then the mixed liquid was loaded into the mold and placed in a vacuum environment to degas to ensure complete filling. The mold was placed in a drying oven and heated at 60 °C for 6 h. After the PDMS was cross-linked and solidified, the PDMS anchors were taken out of the mold, and cut off the excess part. PDMS anchors were put into 24-well cell culture plates. PDMS mixed liquid was used as an adhesive to connect the anchor to the well plate. They were then placed in a drying oven and heated at 60 °C for 6 h to cross-linking. The manufactured culture platforms were cleaned with absolute ethanol and ultrapure water and then soaked in 75% ethanol solution for disinfection before use.

2.6. Engineered muscle tissue formation

Before constructing engineered muscle tissues, a 4% F-127 solution (P2443, Sigma) was added to the construction platform for 30 min to avoid adhesion of the hydrogel on the platform surface. Discard the F-127 solution, clean the platform with ultrapure water, and let it dry for later use.

C2C12 cells were suspended in a hydrogel mixture (Supplementary table S2). Thrombin was added at a concentration of 2 units per milliliter. And then use a pipette to add 0.3 mL of the mixture to seed the cell/hydrogel in each well of the construction platform. The platform was gently shaken to evenly distribute the mixture inside the platform. Tissues were then incubated for 30 min at 37 °C to expedite thrombin-mediated fibrin polymerization. 0.5 mL growth medium containing 2 mg/mL ACA was added to each well. After 2 days, the growth medium was exchanged to differentiation medium which also contained 2 mg/ml ACA (Fig. 1). This time point was marked as differentiation Day 0 (Fig. 3a). Half of the culture medium was replaced every other day thereafter until the desired experimental endpoint unless otherwise indicated [13].

For the conditioned medium derived from mesenchymal stem cells, unless otherwise specified, it contains 10% FBS and 1% P/S for growth and 2% HS and 1% P/S for different. The culture medium used for engineered tissues contained 2 mg/ml ACA.

2.7. Cell viability tests

As shown of schematic diagram of the timeline for culturing engineered muscle tissues in Fig. 3a. The cell viability was determined on Day −1 and Day 1, and the whole tissues were stained using calcein/PI cell viability/cytotoxicity assay kit (C2015 M, Beyotime) at 37 °C away from light for 30 min. The microscopy images were obtained by Nikon Eclipse Ti 2 fluorescent microscope, observing live (green) and dead (red) cells in the tissues. After that, we counted the number of living cells and dead cells using Fiji software, and the cell viability was calculated by dividing the number of living cells by the sum of the number of living cells and dead cells.

2.8. Myoblast proliferation, survival, and metabolism

The hydrogels in the culture platform were cross-linked. Medium from different sources were added, including (1) growth medium (blank) and (2) conditioned medium from MSCs (MSC-CM). Cell counting kit-8 (CCK-8, CK04, DOJINDO) was used to determine cell proliferation after 48 h. The survival of myoblasts

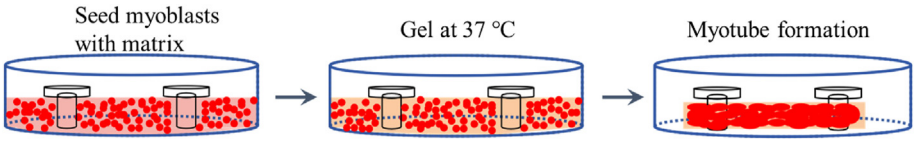

Fig. 1. Automatic tissue formation within platform. Myoblasts are seeded into well in combination with matrix and allowed to gel at 37 °C. Cells subsequently condense around the two elastomeric poles.

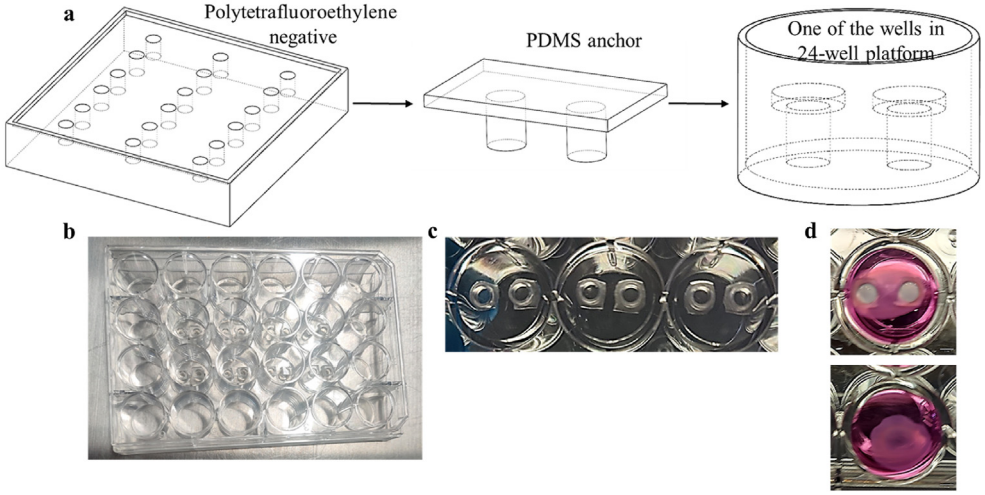

Fig. 2. Design and structure of the culture platform. (a) Culture platform production started with creating a three-dimensional computer aided design (3D CAD) using SolidWorks™ Software which was then made of polytetrafluoroethylene. Next, a various of intermediates were created from the polytetrafluoroethylene negative part. Finally, each intermediate was combined with a 24-well plate, and the excess was cut off to form the final culture platform. (b) Image of culture platform. (c) Image of 3 wells of the culture platform. (d) Tissues were cultured with (up) and without (down) PDMS anchors.

was measured by artificially creating an apoptotic environment. The medium was replaced at Day −1 with GM containing 10 mg/ml ACA to induce apoptosis for 6h (Supplementary figure S2). Then the medium was removed, and the cells were washed twice with calcium-free PBS. GM and the growth conditioned medium were added respectively. Then, Cell proliferation was determined after 24h.

The consumption of glucose per unit time was used to represent the metabolic capacity of muscle tissue. The medium was removed on Day 9 and added fresh blank medium and the conditioned medium respectively. After 24h, the medium was collected, and the glucose content was test using glucose assay kit with o-toluidine (S0201S, Beyotime). In addition, the glucose content in the culture medium before use was detected and used to calculate the glucose consumption of the tissue within 24 h.

2.9. Analysis of cell orientation in tissues

Scanning electron microscope (SEM) was used to analyze the orientation of the cells in the tissues. The tissues were put into a vacuum freeze dryer for dehydration. After sublimation and sputtering, the longitudinal structure of the samples was observed.

2.10. Cell staining and visualization

To observe the orientation of cells in tissues under the action of the PDMS anchors. The tissues were collected on Day 4 for cytoskeleton immunofluorescence imaging. The tissues were fixed in 4% paraformaldehyde at 4 °C overnight and were washed with PBS for three times, and then were permeabilized with 0.1% triton-X 100 in PBS for 30 min at 37 °C. Nonspecific bindings were blocked with 1% bovine serum albumin (BSA, A8010, Solarbio) in PBS for 30 min at 37 °C. The constructs were stained with rhodamine phalloidin (Abcam, ab235138) for 1 h at room temperature, and were washed with PBS for three times, and then were stained with DAPI for 10 min at room temperature. Finally, the tissues were washed with PBS for three times and visualized with Nikon Eclipse Ti 2 fluorescent microscope. To analyze the images, they were converted into highly contrasted 8-bit images and were processed using OrientationJ plugin of Fiji software.

For the tissue staining, the constructs were fixed in 4% paraformaldehyde at 4 °C overnight, and were washed with PBS for three times, and then were permeabilized with 0.5% triton-X100 in PBS for 15 min. Nonspecific bindings were blocked with 5% BSA in PBS for 0.5 h at room temperature. The constructs were stained with anti-sarcomeric alpha actinin antibody (1:200, abcam, ab68167), anti-Pax7 antibody (1:200, abcam, ab187339) and anti-Myog antibody (1:200, abcam, ab77232) at 4 °C overnight, and were washed with PBS for three times, and then were stained with goat anti-rabbit IgG H&L (FITC) (1:1000, abcam, ab6717) for 2 h at room temperature. Rhodamine phalloidin was also used for cytoskeleton immunofluorescence imaging. After rinsed with PBS, cell nuclei were stained with DAPI staining solution (C1005, Beyotime). Images were acquired by using a Nikon Eclipse Ti 2 fluorescent microscope. For the morphometric analysis, myotubes were multinucleated muscle fibers containing at least three nuclei. The width and the area of the myotubes were analyzed using ImageJ software [14].

2.11. Quantitative reverse transcription polymerase chain reaction (RT-qPCR) analysis

The expression levels of myogenic genes of the engineered muscle tissue were evaluated using a one-step RT-qPCR procedure.

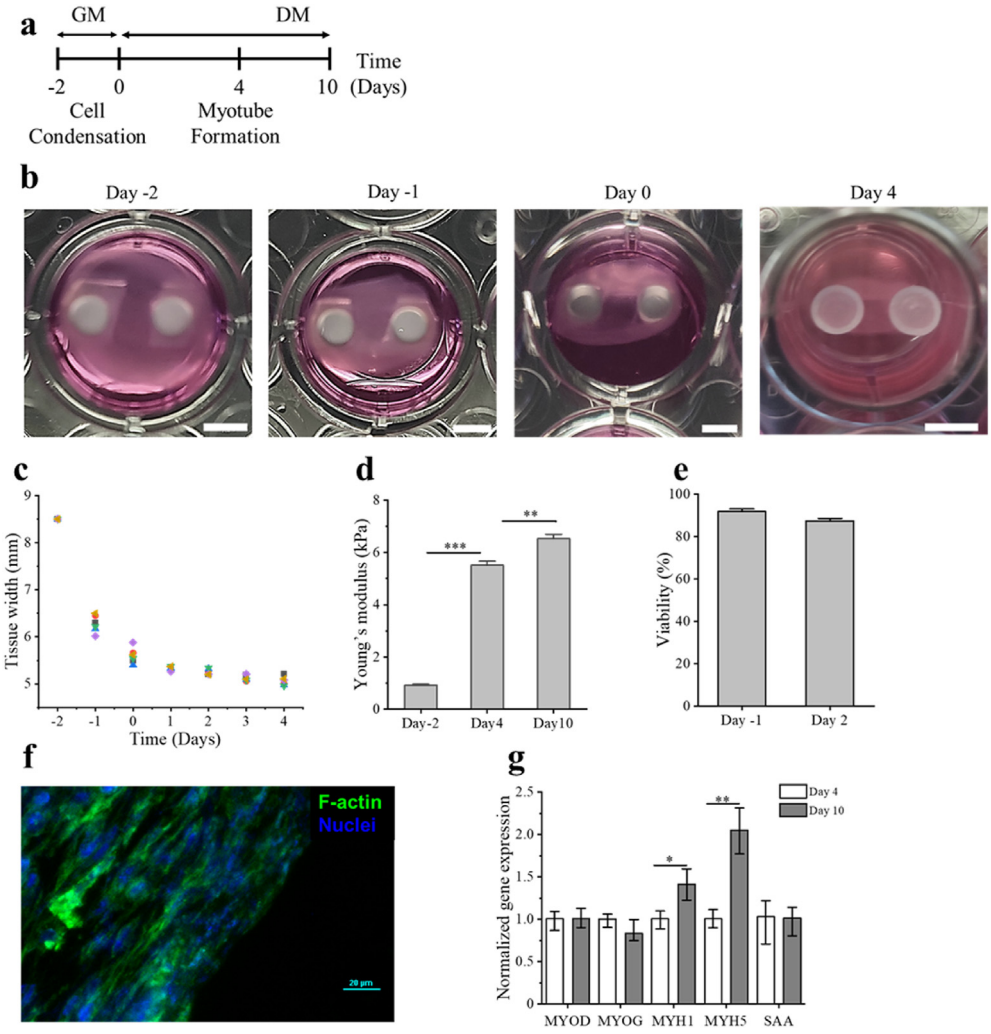

Fig. 3. (a) Schematic diagram of the timeline for culturing engineered muscle tissues. Engineered muscle tissues are cultured in growth medium for the first two days (Day −2 to Day 0), and then the medium is change to differentiation medium on Day 0. (b) Representative phase-contrast images of engineered muscle tissues depicting the remodeling of the matrix by C2C12 over time. Day 0 marks the time for switching to differentiation medium. Scale bar 2 cm. (c) Dot plot indicating the width of engineered muscle tissues over the course of culture (n = minimum of 3 tissues). The width of engineered muscle tissues was defined as the distance from the upper edge to the lower edge of tissues in each well. (d) Average surface Young's modulus culturing on Day −2, Day 4, and Day 10 (n = 3, means ± SD; **p < 0.01, ***p < 0.001). (e) Cell viability at Day −1 and Day 1 (n = 3; means ± SD). (f) Representative confocal stitched image of an engineered muscle tissue on Day 10, stained for F-actin (green) and counterstained with DAPI (blue) to highlight the nuclei. (g) mRNA expression levels of the selected myogenic differentiation markers measured by RT-qPCR for Engineered muscle tissues on Day 4 and Day 10 (n = 3; means ± SD; *p < 0.05, **p < 0.01).

The samples were washed with PBS on Day 4 and Day 10 and then were placed in 800 μl of trizol reagent (15596026, ThermoFisher Scientific). RNA extraction was performed according to the manufacturer's instructions. The concentration and the purity of RNA were tested using Tnano-700, after which the product was diluted with RNase-free water.

The expression levels of the relative myogenic differentiation genes (Myogenin, MYH1, SAA, MyoD, Myf5) were analyzed using SYBR green one-step qRT-PCR kit (D7268S, Beyotime). β-actin was used for internal normalization. Primers for RT-qPCR in this study are listed in Supplementary Table S3. The data analysis followed the following formulas, where the cDNA cycle threshold (CT) values were obtained from the real-time PCR software, and the average CT values from triplicate reactions:

(a) $d\ C_{T(sample,\ gene)} = C_{T(sample,\ gene)} - Average\ (C_{T(sample,\ \beta\text{-actin})})$
(b) $dd\ C_{T(sample,\ gene)} = d\ C_{T(sample,\ gene)} - Average\ ((d\ C_{T(control,\ gene)}))$
(c) $Foldchange = 2^{-}dd\ C_{T(sample,\ gene)}$.

2.12. Statistical analysis

All quantitative data are expressed as means ± standard deviations. In the comparison of two groups of data, a *t*-test was performed to evaluate statistical significance, which was denoted as follows: *p < 0.05, **p < 0.01, ***p < 0.001. Parametric tests included the one-way ANOVA followed by Tukey's multiple comparison test. Statistical analyses were completed using Origin2021 (Origin Lab, USA).

3. Results

3.1. Fabrication of a platform for culturing engineered muscle tissue

The platform is derived from a classic solution and redesigned in this study to support a simple and reproducible culture of engineered muscle tissues [15]. The platform is prepared based on 24-well cell culture plates in which each well consists of an inner

chamber containing two vertical anchors at either end (Supplementary figure S1).

This configuration ensures that the culture of engineered muscle tissue did not require complex equipment. A multi-step casting process is employed to fabricate the culture platform (Fig. 2a), resulting in the creation of a reusable PTFE negative mold. This mold enables the reproducible generation of culture platforms through a multi-step polydimethylsiloxane (PDMS) casting process within a short time (Fig. 2b). The T-shaped feature at the top of each anchor is a key design to inhibit tissues migrate from anchors during culture process (Fig. 2c).

Three-dimensional (3D) engineered muscle tissues were cultured by using mouse C2C12 myoblasts suspended in a hydrogel (Supplementary Table S2) based on a previously published work [16]. The cell-hydrogel suspension was pipetted into the well chambers. The anchors in each well act as tendon-like anchor points. They establish uniaxial tension in the engineered muscle tissue during remodeling and guide tissue formation and compaction within the well. (Fig. 2d).

3.2. Culture of engineered muscle tissue in platform

At first, formation of engineered muscle tissues was investigated over time (Fig. 3a). The scheme was formulated with reference to the previous work experience [17]. Engineered muscle tissues were remodeled within two days of culture in growth medium and continued to compact over the next 10 days (Fig. 3a–d). This process was reflected in the shape of the cells in the tissue and the width of the tissue. All the tissues showed the highest rate of shrinkage from Day −2 to Day −1 (the width of tissues reduced from 8.5 mm to 6.5 mm approximately) (Fig. 3c). Then, the shrinkage rate gradually decreased and reached equilibrium by Day 4. Young's modulus of the tissue at two-time points also reflected the compaction process of the tissue (Fig. 3d). The local Young's modulus was roughly 0.8 kPa in Day −2. After 12 days of culture, the tissues reached a Young's modulus of 6.3 kPa, which was approximately 8-fold higher. Finally, LIVE/DEAD and DAPI staining were used to visualize the cells and evaluate the viability on Day −1 and Day 1, and the staining showed that a high viability of 90% (Fig. 3e and Supplemental figure S3).

On Day 10 after changing the differentiation medium, engineered muscle tissue was observed to form multi-nucleated and aligned myotubes just like Fig. 3f, and was evaluated by immunofluorescence staining against SAA in Supplementary figure S4B. Finally, the structure of tissues gradually matured, which was confirmed by the gradual increase in gene expression (Fig. 3g). MYH is a protein expressed in the final stage of myoblast differentiation. With the culture time progressed, the expression of MYH gene gradually increased, while SAA (a muscle-specific marker highly expressed in fully differentiated myotubes) protein expression remained relatively steady over time.

3.3. Characterization of muscle cell arrangement

In order to assess the effectiveness of our platform in the biofabrication of engineered muscle tissue, we compared the tissues cultured with and without the platform on Day 0. We observed the surface structures of the tissues by cryo-SEM microscopy. The surface of the tissues cultured with the platform showed an oriented fibrin alignment on Day 0. Others were observed the compaction of the hydrogel (Fig. 4a). Despite having the same matrix composition and cell density, these tissues differed significantly in their 3D architecture (Fig. 4b). Tissues which cultured in the platform were characterized by a remarkable aligned

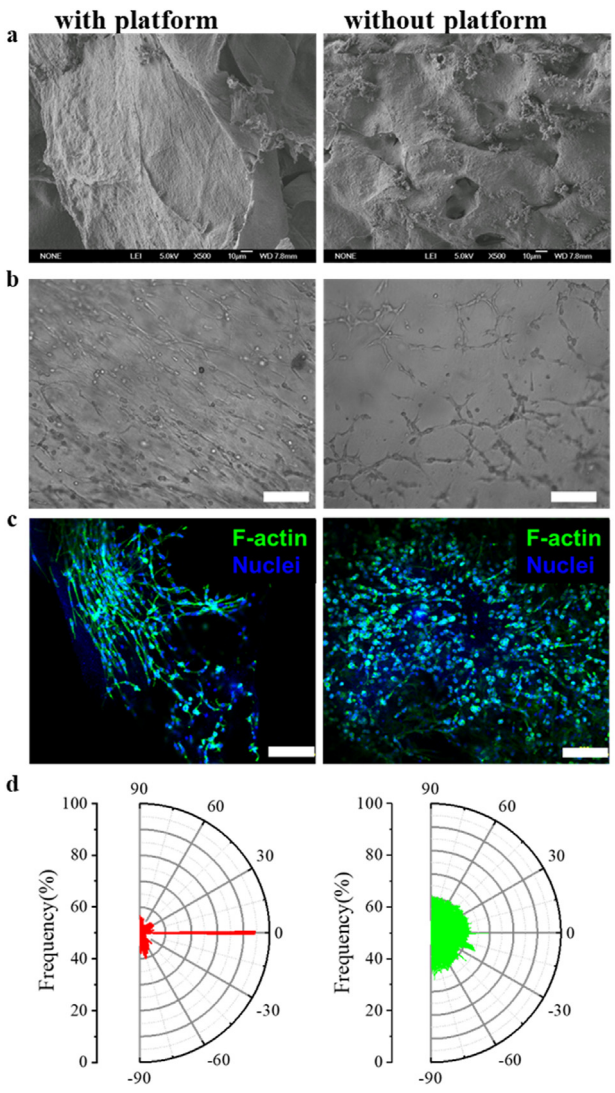

Fig. 4. Comparison of the orientation of the cells and fibrin fibers which cultured with the platform (left) and without the platform (right) on Day 4. (a) SEM images of the surface of engineered muscle tissues, scale bar: 10 μm. (b) The representative images of bright field images, scale bar: 200 μm. (c) Immunofluorescence images of F-actin stained with phalloidin (green) and a nuclear counterstain with DAPI (blue), scale bar: 200 μm. (d) Quantification frequency of cell orientation (n = 3).

architectural organization. Others showed an entangled, disordered cell layout.

The cytoskeletons of tissues were evaluated by immunofluorescence staining (phalloidin) on Day 4. This revealed a substantial parallel organization of myotube and an entangled, disordered myotube layout (Fig. 4c). Myotube organization was further analyzed quantitatively through fluorescent image analysis. As shown in the polar plots in Fig. 4d, more than 80% myotubes in the platform were aligned with the fiber orientation. Whereas those cultured without the platform, the myotube orientation was random with no preferential direction.

3.4. MSCs conditioned medium enhances tissue cell viability

The potential effects of bioactive factors derived from rat mesenchymal stem cells on myoblasts (C2C12) was examined by exposing engineered muscle tissues to the conditioned medium. Assessment of the growth dynamics of myoblasts via the number of myoblasts showed higher proliferation rates for C2C12 cells grown

in MSC conditioned medium (MSC-CM = 1.35, relative to blank = 1.000) (Fig. 5a). The number of myoblasts was counted by a CCK-8 cell counting assay kit. In addition, 6-aminocaproic acid solution (10 mg/ml) was added to the culture medium on the Day −1 of tissue culture to create an apoptotic environment artificially. The anti-apoptotic benefits of MSC-derived paracrine factors were validated. This analysis revealed significantly improved survival of cells cultured in MSCs conditioned medium (1.2-fold) compared to its counterparts grown in the blank medium (Fig. 5b).

For further investigation of the paracrine effects of MSCs on engineered muscle tissue function, we compared the metabolism potential of tissues depending on the culture conditions. Glucose consumption in engineered muscle tissue was measured over 24 h on Day 10 and glucose metabolism of the cells cultured by conditioned medium was increased as shown by decreased medium concentration of glucose (Fig. 5c). In contrast, immunophenotyping of the relevant myogenic differentiation genes demonstrated that the expression of myogenic differentiation (MyoD), myosin heavy chain (MYH1 and MYH5) and myogenin (myog) genes in the MSC-CM was higher than in the blank group, suggesting the terminal differentiation of C2C12 cells in the MSC-CM group (Fig. 5d).

These results indicate that paracrine factors secreted from MSCs promote the proliferation and survival of C2C12 myoblasts, while increased the metabolism and differentiation of tissues.

3.5. MSCs conditioned medium promotes growth and structural maturation of tissues

To investigate the promotion of the engineered muscle tissue, MSC-CM was used to engineered muscle tissue that had been grown and differentiated for the whole culture cycle. Tissues were collected and analyzed by immunohistology on Day 10 and used to study the effect of the mesenchymal stem cell conditioned medium on myotube maturation in engineered muscle tissue. The visual observations showed that the cells cultured in conditioned medium were more mature in Fig. 6a.

The visual observations indicated that the cells cultured in the conditioned medium were more mature in Fig. 6a. The immunofluorescence analysis revealed that tissue differentiation occurs in the presence of MSC-CM, resulting in tissues with higher cell density and larger myotube dimensions. The statistical analysis demonstrated that the myotube length, diameter, and area in the conditioned medium were better than those in the blank medium (Fig. 6b). The average lengths of the myotubes cultured in the blank medium and the MSC-CM were 200 μm and 230 μm, their average diameters were 12 μm and 14 μm; and their average areas were 2700 μm^2 and 3000 μm^2, respectively.

In addition, tissues were taken out from the platform and the expression levels of differentiation proteins paired box gene 7 protein (Pax7) and myogenin (Myog) corresponding to different differentiation nodes of each tissue were directly detected by immunohistochemistry. As shown in Fig. 7. (a) and (b), the addition of conditioned medium can increase the density of cells in the tissue (Fig. 7. (c)). In the conditioned medium, the two differentiation proteins had higher positivity (Fig. 7. (d)). The characterization results of RT-qPCR in Fig. 5d and immunohistochemistry also show that conditioned medium can effectively increase the expression of cell myogenic differentiation proteins. These results suggest that conditioned medium is beneficial to cell differentiation.

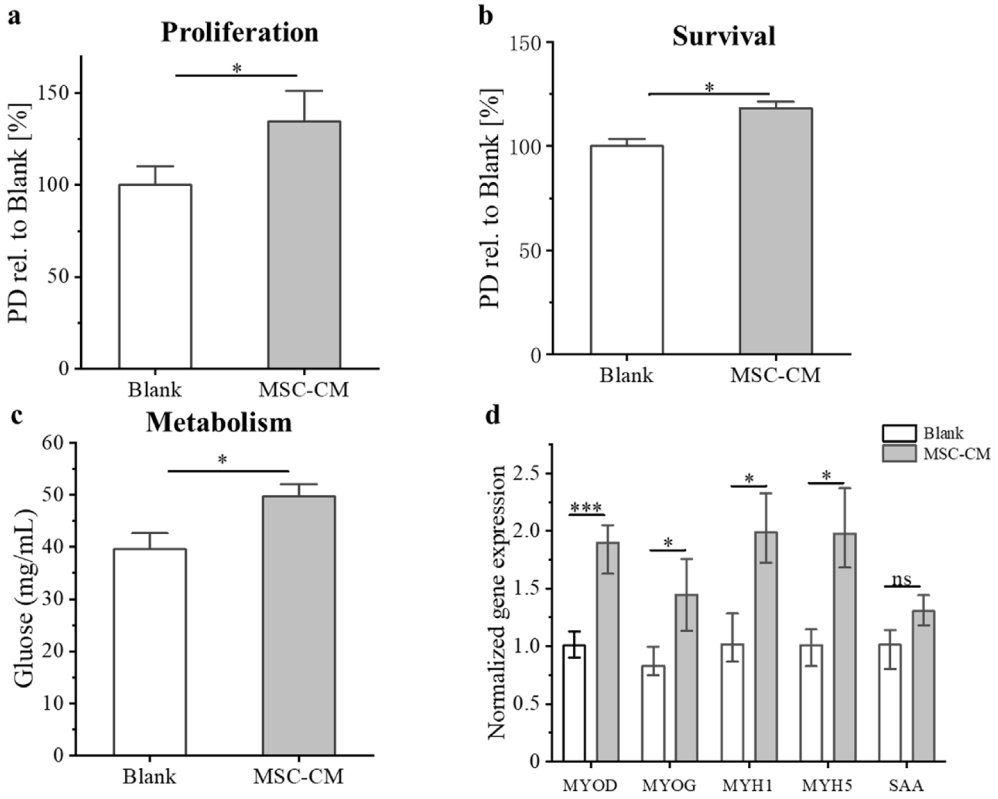

Fig. 5. Paracrine factors from MSCs in conditioned medium influence myoblast function. Conditioned medium from MSCs enhance C2C12 proliferation (a), survival (b) (n = 4; means ± SD; *p < 0.05). (c) The decreased concentration of glucose in medium following 24 h culture of 12-day-old tissues; (n = 3; means ± SD; *p < 0.05). (d) Quantified mRNA expression of the myogenic differentiation related genes on Day 10 (n = 3; mean ± S.D, *p < 0.05, ***p < 0.001, ns = not significant).

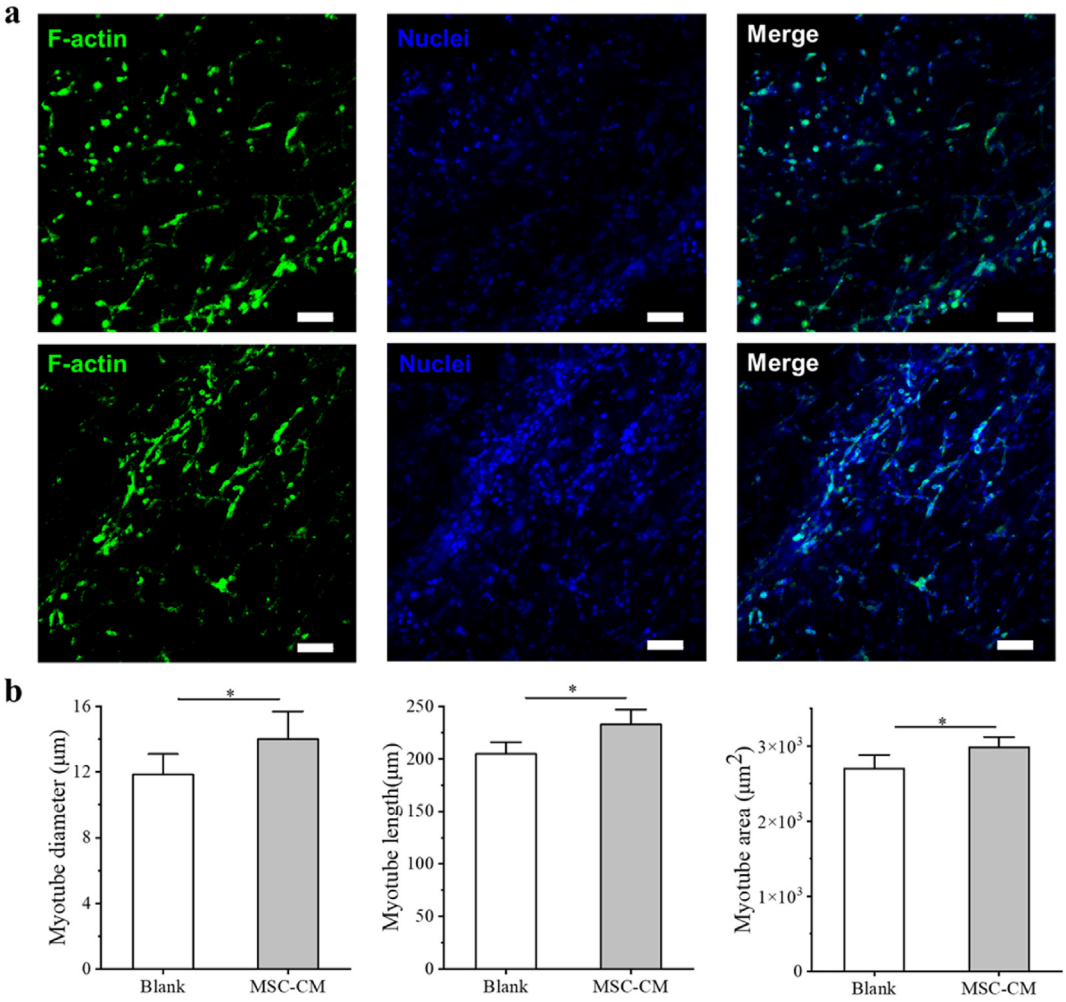

Fig. 6. Immunofluorescence micrographs and statistics for myotube maturity in the C2C12 cells at different groups. Representative immunofluorescence image of a sample on Day 10 stained for F-actin (green) and DAPI for nuclear counterstain (blue). Scale bar: 100 μm. (a) Tissues cultured with Blank medium and MSC-CM. (b) Quantification of myotube diameter, length, and area on Day 10 (n = 3; means ± SD; *p < 0.05).

4. Discussion

Here we report a simple and convenient design of a construction platform for engineered muscle tissue based on a 24-well culture plate. The platform relies on typical anchor structures for tissue formation and design refers to some typical designs [8,18,19]. The anchor specifications have been redesigned and iterated to adapt to 24-well cell culture plates. PDMS anchors on the platform mimic the function of tendons in skeletal muscle development. During the formation of skeletal muscle tissue, the anchors serve as mechanical boundary constraints. These constraints direct cellular contractile forces along the longitudinal axis of the nascent muscle [18,20–22]. Each well of the culture platform contains a cell seeding chamber and two vertical anchors, supporting engineered muscle tissues formed via rapid contraction in less time, which are lassoed around the anchors [23]. An important detail is the initial circular geometry of the cell seeding gel, which effectively preventing necking in the central regions of sculpted tissues tethered under tension. Necking has been reported as a mode of structural failure in engineered tissue constructs under tension [24].

Although in current research work, a variety of culture platforms based on mold-forming principles have been developed and have achieved certain results in applications such as disease modeling [25]. For example, Francisca M used a platform designed based on the anchors to construct engineered muscle tissue and studied the interaction between muscle and fat in vitro [26]. However, the fabrication of this platform requires both a cast PDMS substrate and specially treated metal anchors. In addition, the PDMS substrate of this platform is small, and the culture medium needs to be replaced more frequently during tissue culture. This not only increases the workload of researchers, but the uncertainty in the operation process also increases the risk of tissue culture failure. We developed a reusable PTFE mold that can be employed to cast many PDMS anchors in a single step. The 24-well plates, which are currently widely used for laboratory cell culture, were directly used as the structural unit of the culture substrate. This is an extra advantage of using a 24-well culture plate as the basis for an engineered muscle tissue culture platform. In the specific context of muscle tissue engineering, a variety of advanced technologies, such as 3D bioprinting or electrospinning have been implemented [16,29]. However, there is no doubt that these technologies have many shortcomings such as difficulties in equipment manufacturing and complex tissue culture. All in all, the culture platform makes engineered muscle tissue production fast, low-cost, and user-friendly.

During the cell culture process, the cell loaded hydrogel formed an internal structure like muscle bundles due to the spatial constraints of imposed by PDMS anchors. When myoblasts start to exert an isotropic contractile force on the hydrogel, the anchored

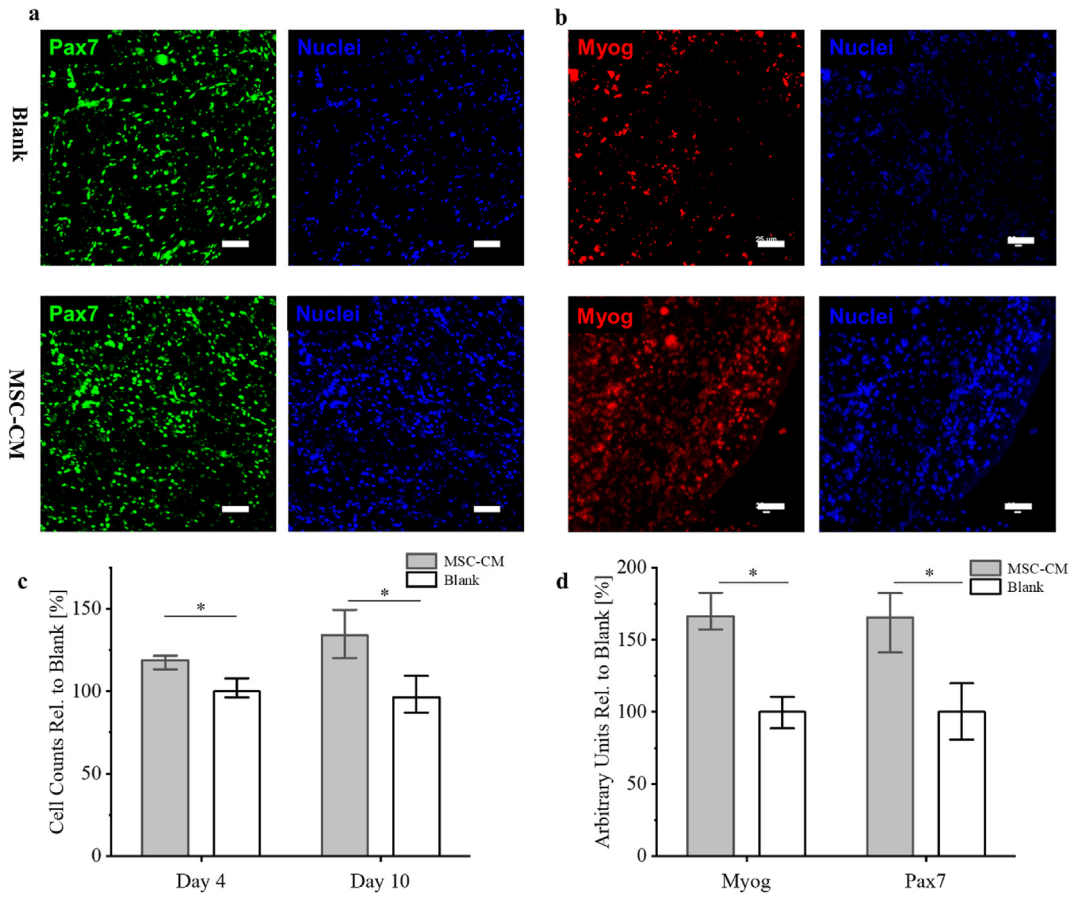

Fig. 7. Representative images of tissues stained for nuclei (blue) and paired box gene 7 protein (Pax7, green) on Day 4 (a), myogenin (Myog, red) and nuclei (blue) on Day 10 (b). Scale bar: 50 μm. Statistical results of cell counts (c), and arbitrary units (d) were quantified using Fiji software. (n = 4; means ± SD; *p < 0.05).

micropillars generate a passive tension, restricting the cell compaction process along the longitudinal direction [20]. In contrast, cells cultured without anchorage exhibited inward collapse and aggregated into cell clusters. On the other hand, cells cultured in the presence of pillars displayed an evident alignment after 2 days. Moreover, as confirmed by immunofluorescence images, aligned initial multinucleated myotubes were observed after differentiation.

Despite the implementation of various technologies for culturing engineered muscle tissues, the maturation and functions of skeletal muscles have only been partially recapitulated in vitro. These approaches, although promising, are still far from satisfactorily addressing the key challenge of muscle tissue engineering, the development of macroscopic tissue equivalents of a size suitable for treating VML [27]. A contributing factor is that in vitro cultures cannot simulate the complex physiological environment of in vivo musculature. The therapeutic application of beneficial cell treatments, such as mesenchymal stem cell therapy can greatly enhance the rate of regeneration of damaged muscle tissue [28]. Indeed, increasing evidence suggests that the tissue restoration function of mesenchymal stem cells is not regulated by their differentiation capability but by the paracrine effects of their soluble factors [29,30]. Roberta demonstrated the capability of mesenchymal stem cell conditioned medium to attenuate EC-induced tissue structural damages and sarcopenic functional properties' modifications, and it was effective in protecting myofibers from apoptosis [31]. In addition, three typical trophic factors such as IGF and HGF in the conditioned medium were detected using Elisa, and their concentrations are shown in Supplementary Table S4. These factors have been shown to have significant effects on promoting muscle differentiation. For example, the injection of appropriate doses of IGF into animals with muscle damage can enhance muscle fiber regeneration and protect cells from apoptosis [32]. And HGF signals through SHP2 in myoblasts and satellite cells to directly alter proliferation rates [33].

Therefore, we also believe that the conditioned medium derived from mesenchymal stem cells is beneficial to culture engineered muscle tissue. In addition, mesenchymal stem cells were cultured on the surface of microcarriers and used to extract conditioned medium. The utilization of microcarriers for culturing cells could increase the cell seeding density per unit volume of culture medium, the proliferation and paracrine rate of mesenchymal stem cells cultured on the surface of microcarriers with suitable properties was also improved [34]. Thereby improving the concentration of factors in the conditional medium [35]. Skeletal muscle hypertrophy in vivo occurs through two primary mechanisms: 1) increased satellite cell activation, proliferation, and fusion into pre-existing or new myofibers, and 2) increased net protein synthesis in mature myofibers [36]. According to these findings, we found that the conditioned medium improved the proliferation and metabolic capacity of myogenic cells in tissues, which is a phenomenon that has been previously reported in animal experiment of mesenchymal stem cell therapy [29].

Skeletal muscle cells require hundreds to thousands of nuclei within a shared cytoplasm for proper function. This increased cell density inessential for engineered muscle tissue [37]. Additionally, conditioned medium can enhance the net protein synthesis, as evidenced by the increased expression of related genes. A variety of

late differentiation genes of myogenic cells, such as MYH, exhibit higher expression levels in tissues cultured by the conditioned medium. Furthermore, the maturity of muscle tissue can be reflected by the status of myotubes [38]. Through immunochemistry staining and data statistics, we found that the muscle tissues in the conditioned medium group had the higher values for the diameter and the area of myotubes. Therefore, the introduction of mesenchymal stem cell conditioned medium into the culture system can improve the maturation of engineered muscle tissue. While we did not evaluate the dynamic force of muscle fibers, the higher glucose utilization rate represents a more mature development of muscle tissue function, which may provide valuable insights for future construction of engineered muscle tissue [39].

Previous research has shown that mesenchymal stem cells can practically secrete cytokines that can modulate the physiological activities of myocytes, thereby improving muscle tissue regeneration. The diameter of the muscle fibers we cultured reaches 14 μm, approximately 20% higher than those produced by conventional culture methods. However, compared with the muscle fibers of living organisms that are several millimeters or even centimeters long, the length of engineered muscle tissues cultured with conditioned medium was far insufficient.

The prerequisite for myotube fusion and muscle fiber elongation is the presence of a sufficient number of myogenic cells in the tissue. Due to the limitation of mass transfer obstacles, it is impossible to further increase the cell density inside the tissue when constructing engineered muscle tissue [40]. The increase in cell density in muscle tissue leads to a corresponding increase in the consumption of nutrients. However, the corresponding rate of mass transfer does not increase accordingly. This results in cells within the tissue not receiving sufficient nutrients, leading to apoptosis. Mesenchymal stem cell conditioned medium promotes proliferation and resists apoptosis of myoblasts, which is an indirect means to increase cell density in tissues. However, in order to further increase the cell density and volume of tissues, the mass transfer problem of tissues needs to be solved. The transport of nutrients in the human body relies on the vascular network spread throughout skeletal muscle tissue. The current method to solve this problem is to construct a vascular network in engineered muscle tissue in vitro to deliver nutrients and metabolic waste. This will be our future research direction.

5. Conclusion

In summary, we have demonstrated a PDMS anchor platform adapted for a 24-well cell culture plate to fabricate engineered muscle tissues, enhanced by mesenchymal stem cell-conditioned medium to promote tissue maturity. Utilizing immunofluorescence staining, cryo-electron microscopy, and quantitative PCR, we systematically observed the fusion, maturation, differentiation, and alignment of C2C12 cells in a fibrin hydrogel system. Further evaluations of cell viability, gene expression, and myotube characteristics reinforced the beneficial impact of the conditioned medium on myotube maturation. Collectively, our results highlight the significant potential of these straightforward and accessible methodologies in constructing and maturing engineered muscle tissues, presenting a viable strategy for the restoration of damaged skeletal muscle. This research contributes meaningfully to the advancement of muscle tissue engineering.

Authorship contribution

Yihao Wen: Writing – original draft, Visualization, Methodology, Data curation. **Jia Tian:** Methodology, Investigation, Conceptualization. **Juan Li:** Formal analysis, Data curation. **Xiangming Na:** Formal analysis, Data curation. **Ziyi Yu:** Writing – review & editing, Supervision, Project administration. **Weiqing Zhou:** Writing – review & editing, Supervision, Project administration, Funding acquisition. All authors read and approved the final manuscript.

Funding

This work is supported by National Key Research and Development Program (2020YFA0112603, 2021YFC2102802).

Availability of data and materials

The datasets generated and analyzed during the current study are available from the corresponding author on reasonable request.

Declaration of competing interest

All authors disclosed no relevant relationships.

Appendix A. Supplementary data

Supplementary data to this article can be found online at https://doi.org/10.1016/j.reth.2024.08.011.

References

[1] Blaauw B, Reggiani C. The role of satellite cells in muscle hypertrophy. J Muscle Res Cell Motil 2014;35:3–10.
[2] Dumont NA, Bentzinger CF, Sincennes MC, Rudnicki MA. Satellite cells and skeletal muscle regeneration. Compr Physiol 2015;5:1027–59.
[3] Grogan BF, Hsu JR, Consortium STR. Volumetric muscle loss. JAAOS - Journal of the American Academy of Orthopaedic Surgeons 2011;19:S35–7.
[4] Stern-Straeter J, Riedel F, Bran G, Hoermann K, Goessler UR. Advances in skeletal muscle tissue engineering. in vivo 2007;21:435–44.
[5] Rossi CA, Pozzobon M, De Coppi P. Advances in musculoskeletal tissue engineering: moving towards therapy. Organogenesis 2010;6:167–72.
[6] Rousseau E, Raman R, Tamir T, Bu A, Srinivasan S, Lynch N, et al. Actuated tissue engineered muscle grafts restore functional mobility after volumetric muscle loss. Biomaterials 2023;302:122317.
[7] Development and Progress of Engineering of Skeletal Muscle Tissue. Tissue Engineering Part B: Reviews 2009;15:319–31.
[8] Afshar ME, Abraha HY, Bakooshli MA, Davoudi S, Thavandiran N, Tung K, et al. A 96-well culture platform enables longitudinal analyses of engineered human skeletal muscle microtissue strength. Sci Rep 2020;10:6918.
[9] Chen Z, Zhao R. Engineered tissue development in biofabricated 3D geometrical confinement–A review. ACS Biomater Sci Eng 2019;5:3688–702.
[10] Madden L, Juhas M, Kraus WE, Truskey GA, Bursac N. Bioengineered human myobundles mimic clinical responses of skeletal muscle to drugs. Elife 2015;4:e04885.
[11] Mueller C, Trujillo-Miranda M, Maier M, Heath DE, O'Connor AJ, Salehi S. Effects of external stimulators on engineered skeletal muscle tissue maturation. Adv Mater Interfac 2020;8.
[12] Goh Q, Dearth CL, Corbett JT, Pierre P, Chadee DN, Pizza FX. Intercellular adhesion molecule-1 expression by skeletal muscle cells augments myogenesis. Exp Cell Res 2015;331:292–308.
[13] Fan T, Wang S, Jiang Z, Ji S, Cao W, Liu W, et al. Controllable assembly of skeletal muscle-like bundles through 3D bioprinting. Biofabrication 2021;14.
[14] Costantini M, Testa S, Mozetic P, Barbetta A, Fuoco C, Fornetti E, et al. Microfluidic-enhanced 3D bioprinting of aligned myoblast-laden hydrogels leads to functionally organized myofibers in vitro and in vivo. Biomaterials 2017;131:98–110.
[15] Williams ML, Kostrominova TY, Arruda EM, Larkin LM. Effect of implantation on engineered skeletal muscle constructs. J Tissue Eng 2013;7:434–42.
[16] Helfer A, Bursac N. Frame-hydrogel methodology for engineering highly functional cardiac tissue constructs. Methods Mol Biol 2021;2158:171–86.
[17] Shi N, Li Y, Chang L, Zhao G, Jin G, Lyu Y, et al. A 3D, magnetically actuated, aligned collagen fiber hydrogel platform recapitulates physical microenvironment of myoblasts for enhancing myogenesis. Small Methods 2021;5:e2100276.
[18] Mills RJ, Parker BL, Monnot P, Needham EJ, Vivien CJ, Ferguson C, et al. Development of a human skeletal micro muscle platform with pacing capabilities. Biomaterials 2019;198:217–27.
[19] Ebrahimi M, Lad H, Fusto A, Tiper Y, Datye A, Nguyen CT, et al. De novo revertant fiber formation and therapy testing in a 3D culture model of Duchenne muscular dystrophy skeletal muscle. Acta Biomater 2021;132:227–44.

[20] Eyckmans J, Chen CS. 3D culture models of tissues under tension. J Cell Sci 2017;130:63–70.
[21] Furuhashi M, Morimoto Y, Shima A, Nakamura F, Ishikawa H, Takeuchi S. Formation of contractile 3D bovine muscle tissue for construction of millimetre-thick cultured steak. npj Science of Food 2021;5:6.
[22] Shima A, Morimoto Y, Sweeney HL, Takeuchi S. Three-dimensional contractile muscle tissue consisting of human skeletal myocyte cell line. Exp Cell Res 2018;370:168–73.
[23] Legant WR, Pathak A, Yang MT, Deshpande VS, McMeeking RM, Chen CS. Microfabricated tissue gauges to measure and manipulate forces from 3D microtissues. Proc Natl Acad Sci USA 2009;106:10097–102.
[24] Wang H, Svoronos AA, Boudou T, Sakar MS, Schell JY, Morgan JR, et al. Necking and failure of constrained 3D microtissues induced by cellular tension. Proc Natl Acad Sci USA 2013;110:20923–8.
[25] Osaki T, Uzel SGM, Kamm RD. Microphysiological 3D model of amyotrophic lateral sclerosis (ALS) from human iPS-derived muscle cells and optogenetic motor neurons. Sci Adv 2018;4:eaat5847.
[26] Acosta FM, Howland KK, Stojkova K, Hernandez E, Brey EM, Rathbone CR. Adipogenic differentiation alters properties of vascularized tissue-engineered skeletal muscle. Tissue Eng 2021;28:54–68.
[27] Jiang Y, Torun T, Maffioletti SM, Serio A, Tedesco FS. Bioengineering human skeletal muscle models: recent advances, current challenges and future perspectives. Exp Cell Res 2022;416:113133.
[28] Bushkalova R, Farno M, Tenailleau C, Duployer B, Cussac D, Parini A, et al. Alginate-chitosan PEC scaffolds: a useful tool for soft tissues cell therapy. Int J Pharm 2019;571:118692.
[29] Pumberger M, Qazi TH, Ehrentraut MC, Textor M, Kueper J, Stoltenburg-Didinger G, et al. Synthetic niche to modulate regenerative potential of MSCs and enhance skeletal muscle regeneration. Biomaterials 2016;99:95–108.
[30] Zeng M, He Y, Yang Y, Wang M, Chen Y, Wei X. Mesenchymal stem cell-derived extracellular vesicles relieve endothelial cell senescence via recovering CTRP9 upon repressing miR-674-5p in atherosclerosis. Regenerative Therapy 2024;27:354–64.
[31] Squecco R, Tani A, Chellini F, Garella R, Idrizaj E, Rosa I, et al. Bone marrow-mesenchymal stromal cell secretome as conditioned medium relieves experimental skeletal muscle damage induced by ex vivo eccentric contraction. Int J Mol Sci 2021;22:3645.
[32] Borselli C, Storrie H, Benesch-Lee F, Shvartsman D, Cezar C, Lichtman JW, et al. Functional muscle regeneration with combined delivery of angiogenesis and myogenesis factors. Proc Natl Acad Sci U S A 2010;107:3287–92.
[33] Li J, Reed SA, Johnson SE. Hepatocyte growth factor (HGF) signals through SHP2 to regulate primary mouse myoblast proliferation. Exp Cell Res 2009;315:2284–92.
[34] Long R, Wang S. Exosomes from preconditioned mesenchymal stem cells: tissue repair and regeneration. Regenerative Therapy 2024;25:355–66.
[35] Yan X-R, Li J, Na X-M, Li T, Xia Y-F, Zhou W-Q, et al. Mesenchymal stem cells proliferation on konjac glucomannan microcarriers: effect of rigidity. Chin J Polym Sci 2022;40:1080–9.
[36] Costantini M, Testa S, Fornetti E, Fuoco C, Sanchez Riera C, Nie M, et al. Biofabricating murine and human myo-substitutes for rapid volumetric muscle loss restoration. EMBO Mol Med 2021;13:e12778.
[37] Millay DP. Regulation of the myoblast fusion reaction for muscle development, regeneration, and adaptations. Exp Cell Res 2022;415:113134.
[38] Fan T, Wang S, Jiang Z, Ji S, Cao W, Liu W, et al. Controllable assembly of skeletal muscle-like bundles through 3D bioprinting. Biofabrication 2021;14:015009.
[39] Ikeda K, Ito A, Sato M, Kawabe Y, Kamihira M. Improved contractile force generation of tissue-engineered skeletal muscle constructs by IGF-I and Bcl-2 gene transfer with electrical pulse stimulation. Regenerative Therapy 2016;3:38–44.
[40] Gholobova D, Terrie L, Gerard M, Declercq H, Thorrez L. Vascularization of tissue-engineered skeletal muscle constructs. Biomaterials 2020;235:119708.